Gα-Subunits Differentially Alter the Conformation and Agonist Affinity of κ-Opioid Receptors†

Feng Yan,‡ Philip D. Mosier,§ Richard B. Westkaemper,§ and Bryan L. Roth*,‡,||

Department of Biochemistry, Case Western Reserve University, Cleveland, Ohio 44106, Department of Pharmacology, University of North Carolina, Chapel Hill, North Carolina 27599, and Department of Medicinal Chemistry, Virginia Commonwealth University, Richmond, Virginia 23298

Received July 25, 2007; Revised Manuscript Received November 20, 2007

ABSTRACT: Although ligand-induced conformational changes in G protein-coupled receptors (GPCRs) are well-documented, there is little direct evidence for G protein-induced changes in GPCR conformation. To investigate this possibility, the effects of overexpressing Gα-subunits ($G\alpha_{16}$ or $G\alpha_{i2}$) with the κ-opioid receptor (KOR) were examined. The changes in KOR conformation were subequently examined via the substituted cysteine accessibility method (SCAM) in transmembrane domains 6 (TM6) and 7 (TM7) and extracellular loop 2 (EL2). Significant conformational changes were observed on TM7, the extracellular portion of TM6, and EL2. Seven SCAM-sensitive residues ($S310^{7.33}$, $F314^{7.37}$, and $I316^{7.39}$ to $Y320^{7.43}$) on TM7 presented a cluster pattern when the KOR was exposed to baseline amounts of G protein, and additional residues became sensitive upon overexpression of various G proteins. In TM7, $S311^{7.34}$ and $N326^{7.49}$ were found to be sensitive in $G\alpha_{16}$-overexpressed cells and $Y313^{7.36}$, $N322^{7.45}$, $S323^{7.46}$, and $L329^{7.52}$ in $G\alpha_{i2}$-overexpressed cells. In addition, the degree of sensitivity for various TM7 residues was augmented, especially in $G\alpha_{i2}$-overexpressed cells. A similar phenomenon was also observed for residues in TM6 and EL2. In addition to an enhanced sensitivity of certain residues, our findings also indicated that a slight rotation was predicted to occur in the upper part of TM7 upon G protein overexpression. These relatively modest conformational changes engendered by G protein overexpression had both profound and differential effects on the abilities of agonists to bind to KOR. These data are significant because they demonstrate that Gα-subunits differentially modulate the conformation and agonist affinity of a prototypical GPCR.

For many years, it has been clear that GPCR[1] agonists display functional selectivity or the ability of ligands (both agonists and antagonists) to differentially modulate signaling pathways depending on the cellular milieu (*1*−*5*). Since G proteins are heterogeneously distributed in various cell compartments and show cell type and developmental expression patterns (*6*−*8*), it has been suggested that the cellular expression profile of G proteins and effectors will affect the pattern of activation of downstream signaling pathways (*9*−*11*). In fact, recent reviews of the G protein-dependent pharmacology of ligands suggest the promise for designing conformationally selective ligands (*12*) (i.e., ligands that bind preferentially to particular GPCR conformations).

One possible explanation for the phenomenon of functional selectivity is that G proteins differentially shift the conformation of GPCRs from the ground state to a series of activated states. According to this model, different agonist molecules preferentially sample some conformational changes over others, leading to the establishment of an agonist-preferred G protein-coupling pathway. Indeed, G proteins have recently been shown to precouple with receptors specifically before the addition of agonists (*13*, *14*) leading, perhaps, to distinct conformations. Alternatively, agonists have been proposed to induce differential GPCR conformations, which then lead to distinct patterns of G protein-coupling and pathway activation (*15*, *16*). Although it has been reported that G proteins are present in 10−100 molar excess as compared to GPCRs (*13*, *17*), GPCR overexpression likely changes this ratio with the consequence that the percentage of GPCR that is precoupled to G proteins increases (*18*).

In this work, Gα-subunits were overexpressed with the κ-opioid receptor (KOR) to increase the chances for G protein−GPCR interactions (Figure 1). Since opioid receptors are capable of coupling with the pertussis toxin-sensitive Gα-subunits $G_{i/o}$ and the pertussis toxin insensitive G_z and $G\alpha_{16}$ subunits (*19*, *20*), two types of G proteins were chosen for study: $G\alpha_{i2}$, which has demonstrated preferential coupling to KOR, and the promiscuous Gα-subunit $G\alpha_{16}$. The SCAM mutagenesis method has been used previously to interrogate

† This research was supported in part by RO1DA017204 (B.L.R.) and the NIMH Psychoactive Drug Screening Program.

* Corresponding author. Tel.: (919) 966-7535; fax: (919) 843-5788; e-mail: bryan_roth@med.unc.edu.

‡ Case Western Reserve University.

§ Virginia Commonwealth University.

|| University of North Carolina, Chapel Hill.

[1] Abbreviations: GPCR, G protein-coupled receptor; KOR, κ-opioid receptor; hKOR, human KOR; $G\alpha_{16}$ or $G\alpha_{i2}$, heterotrimeric G protein alpha subunit 16 or alpha subunit i2; KOR·$G\alpha_{16}$, κ-opioid receptor with $G\alpha_{16}$ overexpression; KOR·$G\alpha_{i2}$, κ-opioid receptor with $G\alpha_{i2}$ overexpression; TM, transmembrane domain; EL, extracellular loop; IL, intracellular loop; SCAM, substituted cysteine accessibility method; MTSEA, (2-aminoethyl)methanethiosulfonate; HEK, human embryonic kidney.

10.1021/bi701476b CCC: $40.75
Published on Web 01/19/2008

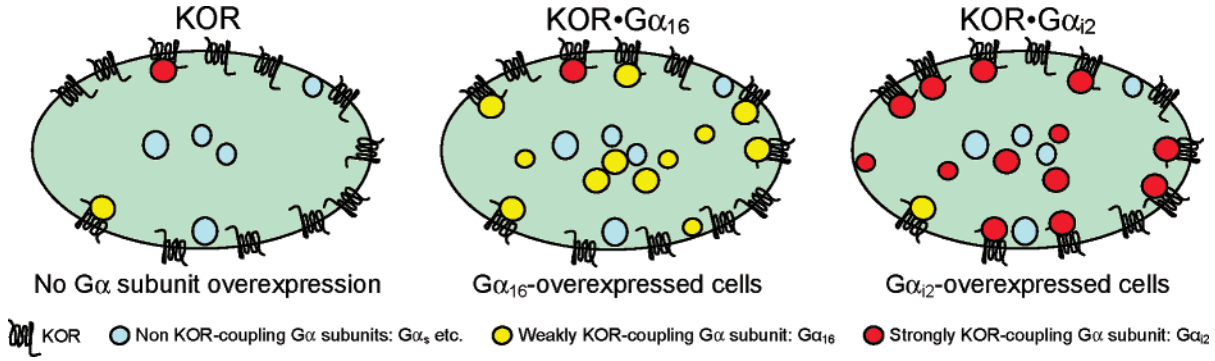

FIGURE 1: Gα-subunit overexpression was used to stabilize receptor conformations in the various active states. In each cell system, KOR exists in both G protein-coupled and uncoupled forms. However, KORs are more likely to be in the G protein-coupled form when G protein alpha subunits (such as $G\alpha_{16}$ and $G\alpha_{i2}$) are overexpressed. For clarification, abbreviations were used to describe the three cell systems: KOR, KOR·$G\alpha_{16}$, and KOR·$G\alpha_{i2}$.

GPCR conformational changes (*21*). Therefore, the SCAM approach was used along with the sulfhydryl reagent (2-aminoethyl)methanethiosulfonate (MTSEA) to probe conformational changes that might occur in TM6, TM7 and EL2 of the KOR in various G protein backgrounds. To our knowledge, this is the first direct evidence that G protein alpha subunits induce different conformational changes in their cognate GPCRs. To our surprise, our results revealed subtle changes in cysteine susceptibility to MTSEA indicative of modest conformational rearrangements upon G protein binding—similar to the modest conformational changes recently reported for rhodopsin upon activation (*22*).

MATERIALS AND METHODS

Materials. [^{3}H]Diprenorphine (54.9 Ci/mmol) and [^{3}H]-U69593 (41.7 Ci/mmol) were purchased from PerkinElmer Life Science, Inc. (Boston, MA). MTSEA was obtained from Anatrace, Inc. (Maumee, OH). Salvinorin A was kindly provided by Dr. Thomas E. Prisinzano (University of Iowa). Naloxone and U69593, together with other standard reagents, were purchased from Sigma-Aldrich (St. Louis, MO). Dynorphin A (1−13) was purchased from both Sigma-Aldrich and Bachem Bioscience, Inc. (King of Prussia, PA). Stable cell lines expressing human $G\alpha_{16}$ and $G\alpha_{i2}$ were obtained by transfecting the G protein expression vectors (pcDNA3.1, UMR cDNA Resource Center) into human embryonic kidney HEK 293 cells and selecting in 900 μg/mL G418. Those cell lines were maintained and transfected in 450 μg/mL G418. The expressions of $G\alpha_{16}$ and $G\alpha_{i2}$ were characterized with anti-human $G\alpha_{16}$ and $G\alpha_{i2}$ polyclonal antibodies (Cell Sciences, Inc., Canton, MA).

Site-Directed Mutagenesis. Site-directed mutagenesis was based on the C315$^{7.38}$S background of the human KOR in the vector pcDNA3.1 following the procedure of the QuikChange mutagenesis kit (Stratagene, Santa Clara, CA). In some situations, FLAG-tagged human wild-type KOR was subcloned into the vector pIRESneo. The presence of the mutations was verified by automated dsDNA sequencing (Genomics Core Facility, Case Western Reserve University, Cleveland, OH) before use.

Transfection of HEK 293T, $G\alpha_{16}$, and $G\alpha_{i2}$ Cells. Cells were grown in 10-cm culture dishes in medium with 10% fetal calf serum in a humidified atmosphere consisting of 5% CO_2 and 95% air at 37 °C. Cells were transfected with either the wild-type, the C315$^{7.38}$S hKOR single mutant, or a double mutant hKOR DNA incorporating the C315$^{7.38}$S mutation (12 μg/10-cm dish) using EasyTransgater (America Pharma Source, Gaithersburg, MD). After a total of 48 h of transfection, cells were harvested for experiments by detaching with Versene solution (Invitrogen, Carlsbad, CA).

Determination of K_d and B_{max} Values for [^{3}H]Diprenorphine Binding. Membranes were prepared from transfected HEK 293T cells. Saturation binding of [^{3}H]diprenorphine to the wild-type and mutant hKOR receptors was performed at eight concentrations of [^{3}H]diprenorphine ranging from 0.03 to 3 nM. Binding was carried out in standard binding buffer (50 mM Tris-HCl, 10 mM $MgCl_2$, and 0.1 mM EDTA, pH 7.4) at room temperature for 1 h in triplicate in a volume of 0.25 mL with about 30 μg of membrane protein. Naloxone (10 μM) was used to define nonspecific binding. Protein contents of membranes were determined by the Bradford protein assay method with BSA as the standard. Binding data were analyzed with Prism 4.03 (GraphPad Software, Inc., San Diego, CA).

MTSEA Reaction. Transfected cells were incubated with Versene solution (2 mL/plate) for 2 min, detached, and pelleted at 1000*g* at 4 °C. After being washed with cold Kreb buffer (130 mM NaCl, 4.8 mM KCl, 1.2 mM KH_2PO_4, 1.3 mM $CaCl_2$, 1.2 mM $MgSO_4$, 10 mM glucose, and 25 mM HEPES at pH 7.4), the pellets were centrifuged and resuspended. The cell suspension was incubated with freshly prepared 1 mM MTSEA in 0.125 mL at room temperature for 5 min. The reaction mixtures were quenched by ice-cold 0.8% BSA Kreb's buffer, then pelleted and washed with regular cold buffer. After centrifugation, the pellets were resuspended, and 100 μL aliquots were used for [^{3}H]-diprenorphine binding.

Radioligand Binding Assays. All assays were conducted in triplicate using standard polypropylene 96-well (8 × 12 format, 1 mL/well) plates (Laboratory Products Sales, Inc., Rochester, NY) as binding reaction containers. Nonspecific binding was defined by 10 μM naloxone prepared in standard binding buffer. Reaction volumes were as follows: 100 μL of standard binding buffer, 25 μL of naloxone (or buffer for total binding), 25 μL of [^{3}H]diprenorphine (0.2 to 0.4 nM final concentration), and 100 μL of membrane receptors. The plates were incubated in the dark at room temperature for 90 min. Filters were presoaked in 0.3% PEI in 50 mM Tris buffer (4 °C, pH 7.4). The binding reaction was terminated by rapid filtration under vacuum by a Brandel harvester. Each

Table 1: K_d and B_{max} Values of [^{3}H]Diprenorphine Binding to Wild-Type KOR and EL2 Cysteine Mutants

EL2 mutants[a]	K_d (nM)	B_{max} (pmol/mg)	$K_{d(mutant)}/K_{d(WT)}$
WT KOR	0.46 ± 0.11	2.7 ± 0.5	
C315S-V205C	0.43 ± 0.07	1.1 ± 0.3	0.9
C315S-D206C	0.29 ± 0.05	0.61 ± 0.28	0.6
C315S-V207C	0.60 ± 0.06	1.0 ± 0.2	1.3
C315S-I208C	0.49 ± 0.10	0.74 ± 0.13	1.1
C315S-E209C	0.63 ± 0.14	0.70 ± 0.14	1.4
C315S-S211C	0.38 ± 0.11	0.83 ± 0.17	0.8
C315S-L212C	0.13 ± 0.04	0.022 ± 0.002	0.3
C315S-Q213 C	0.48 ± 0.03	0.99 ± 0.22	1.0
C315S-F214C	0.24 ± 0.07	0.023 ± 0.002	0.5
C315S-P215C	0.36 ± 0.13	0.39 ± 0.12	0.8
C315S-D216C	0.39 ± 0.08	0.87 ± 0.31	0.8

[a] Saturation binding of [^{3}H]diprenorphine to wild-type and EL2 mutants was performed according to the procedure in Materials and Methods. Data represent mean ± SEM from two to four independent experiments. Receptors are transiently expressed in HEK 293T cells.

well was washed 3 times with cold 50 mM Tris buffer (pH 7.4). Filters were dried and placed into scintillation vials (Laboratory Products Sales, Inc.). To each vial, 4 mL of Ecoscint (biodegradable scintillation solution, National Diagnostics, Atlanta, GA) was added. The scintillation vials were counted in a liquid scintillation counter (PerkinElmer LifeScience, Inc.). The raw data were analyzed by GraphPad Prism 4.03 to determine the inhibition number. The inhibition number was calculated using eq 1

$$\text{inhibition (100\%)} = \left[1 - \left(\frac{K_{spec}(\text{MTSEA}+)}{K_{spec}(\text{MTSEA}-)}\right)\right] \times 100 \quad (1)$$

where K_{spec}(MTSEA+) is the specific binding after the MTSEA reaction and K_{spec}(MTSEA−) is the specific binding without MTSEA. Statistical comparisons were made by one-way analysis of variance (ANOVA) followed by Dunnett's post-test (using $p < 0.01$ as the level of significance).

Determination of Second-Order Rate Constants. The second-order rate constants of the reactions between KOR cysteine mutants and MTSEA was determined (estimated using a pseudo-first-order equation) to gain quantitative information on cysteine sensitivity, according to the published method (*23*, *24*). Cells expressing a KOR mutant receptor were incubated with indicated concentrations of MTSEA (mostly 0.01, 0.25, 1.0, and 2.0 mM) for 5 min. The results were fit to eq 2

$$Y = Ne^{-kct} + \text{plateau} \quad (2)$$

where Y is the fraction of the initial binding, N is the extent of inhibition, k is the second-order rate constant (M^{-1} s^{-1}), c is the concentration of MTSEA (M), t is the incubation time (300 s), and plateau is the fraction of residual binding at saturating concentrations of MTSEA. The data were analyzed by the built-in kinetic function of GraphPad Prism 4.03.

KOR Modeling. Modeling studies were performed using SYBYL (version 7.3, Tripos Associates, Inc., St. Louis, MO). The hKOR model presented here was built using the coordinates of the recently obtained activated bovine rhodopsin crystal (B chain of PDB ID 2I37) (*22*) as the initial template. The coordinates of the atoms in the residues corresponding to the IL2 (N145 to G149) in rhodopsin were merged from the A chain into the B chain. A loop search was performed to replace the missing three residues (A235 to Q237) in the IL3 of rhodopsin, and the IL3 (K231 to A241) was subsequently energy-minimized using the Tripos Force Field (Gasteiger-Hückel charges, distance-dependent dielectric constant = 4.0 and nonbonded cutoff = 8 Å; unless otherwise noted, these parameters remained the same throughout the modeling process). The N- and C-termini of the hKOR were not explicitly modeled; residues representing these regions (M1 to E33 and C322 to P327) were removed. Residues in the structurally conserved transmembrane helical and IL1 regions were mutated to their cognate residues in the hKOR. The rotated extracellular portion of TM2 was incorporated into the model by replacing residues L84$^{2.51}$ to Y102$^{2.69}$ in bovine rhodopsin with residues A106$^{2.51}$ to S123$^{2.68}$ from a previously described TM2-rotated hKOR-salvinorin A interaction model (*25*). The importance of Q115 as a probable H-bonding interaction site for salvinorin A was incorporated into this TM2-rotated hKOR model. This was accomplished by modifying torsion angles in the Q115 side chain followed by unconstrained energy minimization with the Tripos Force Field. The resulting receptor−ligand complex remained essentially unchanged but with a significant hydrogen-bonding interaction between the furan oxygen of salvinorin A and the amide nitrogen of the Q115 side chain. Loop searches were then performed to replace the remaining bovine rhodopsin segments in the model with hKOR segments. The sequence was renumbered, and SCWRL (*26*) version 3 was used to place the side chains onto the hKOR model backbone.

To reproduce the characteristic features of the binding site in the previously described hKOR model (*25*) in which the agonist salvinorin A was bound, additional refinement of the model was carried out. First, to accommodate the ligand in the binding site, EL2 was raised out of the binding cavity, enlarging it. This was accomplished by replacing EL2 (S192 to W221) with the one from the previously described hKOR model (*25*, *27*), in which molecular dynamics (MD) was used to enlarge the binding site cavity. Additionally, to reorient Y313$^{7.36}$ and Y320$^{7.43}$ for consistency with the previously proposed salvinorin A-hKOR interaction model, the coordinates of the atoms in the extracellular portion of TM7 (L309$^{7.32}$ to N322$^{7.45}$) were replaced with the coordinates of the corresponding residues in the earlier hKOR model (*25*).

Next, the side chain conformations of key residues in the hKOR were modified to match those in the rhodopsin template, as these side chains had been assigned conformations by SCWRL that differed significantly from those of the original bovine rhodopsin template. The χ_1 and χ_2 torsion angles of Y330$^{7.53}$ in the NPxxY motif were readjusted to place the side chain in a position to interact with the F337$^{7.60}$ side chain. As a result of this change, the χ_1 torsion angles of I98$^{2.43}$ and Y97$^{2.42}$ were also modified to match those of the cognate residues in the B chain of 2I37. This placed the side chain of Y97$^{2.42}$ in a position to hydrogen bond with the side chain of D155$^{3.49}$ of the D/ERY motif. The χ_2 torsion angles of N77$^{1.50}$, N141$^{3.35}$, and N326$^{7.49}$ were adjusted for optimal hydrogen-bonding interactions with D105$^{2.50}$, thus placing these residues in positions corresponding to those observed in the activated rhodopsin crystal structure and further stabilizing the intracellular helical bundle. As a final

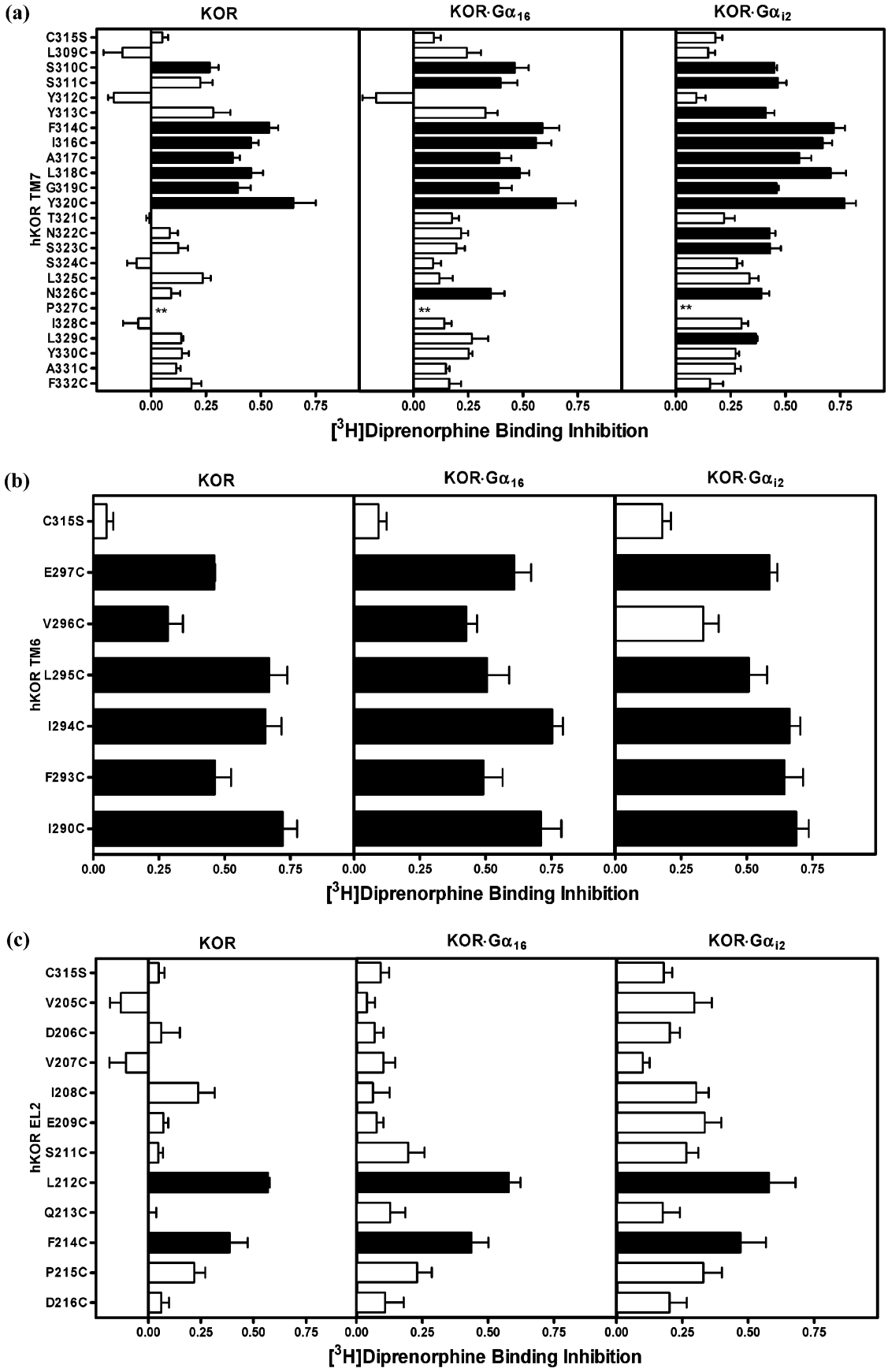

FIGURE 2: (a) SCAM analysis revealed differential MTSEA accessibility patterns in TM7 of the KOR upon various G protein-coupling conditions. MTSEA (1 mM for 5 min) was used to react specifically with cysteine side chains, and the modified cysteines show different inhibitions of [^{3}H]diprenorphine (~0.2 nM) binding. The effects of MTSEA pretreatment on [^{3}H]diprenorphine binding were expressed as inhibition number. Each point represents the mean ± SEM of three to six experiments. Black bars indicate mutants for which inhibition numbers were significantly different ($p < 0.01$) from the reference (C315$^{7.38}$S) by ANOVA and Dunnett's test. (b) SCAM analysis of the upper part of TM6. (c) SCAM analysis of EL2. **: [^{3}H]Diprenorphine binding was undetectable for the C315$^{7.38}$S-P327$^{7.50}$C mutant.

step in the refinement of the hKOR, the agonist salvinorin A was placed into the binding site in a manner previously described (*27*), and the receptor−ligand complex was energy-minimized without constraints. The stereochemical integrity of the final hKOR receptor model was verified by PROCHECK and the ProTable facility within SYBYL 7.3.

RESULTS

Creation of a Large Number of Cys Mutants in TM6, TM7 and EL2 of KOR. Prior to performing cysteine-accessibility studies, a large number of cysteine mutants was created. For these studies, 23 consecutive residues in TM7 (not including C315$^{7.38}$), six residues in the upper part of TM6, and 11 residues in EL2 of KOR were mutated to cysteine based on the C315$^{7.38}$S background (*28*). The K_d and B_{max} values using [^{3}H]diprenorphine for TM6 and TM7 cysteine mutants have been previously reported by others (*23*, *24*). Our pattern of results was similar and showed only minor alterations in diprenorphine affinity (data not shown). For EL2 mutants, the K_d and B_{max} values are summarized in Table 1. Relatively minor alterations in K_d values (0.13 to ~0.63 nM) were found, which are similar to wild-type KOR (0.46 nM), while the B_{max} value ranged from 0.022 to 1.1 pmol/mg (Table 1). These results indicate that cysteine mutagenesis does not greatly alter the antagonist binding affinity. The sole exceptions were the P327$^{7.50}$C mutation, which resulted in a nonexpressed receptor protein as judged by radioligand binding studies, and the Y320$^{7.43}$C mutation. Surface biotinylation and anti-FLAG immunoblotting confirmed that the P327$^{7.50}$C mutant was not expressed and that Y320$^{7.43}$C, along with other selected mutants, was expressed on the plasma membrane (data not shown). Taken together, these findings indicate that the examined cysteine mutations do not drastically affect the binding pocket for diprenorphine and that among the mutants evaluated, surface expression is normal.

SCAM Elucidates Potential Conformational Changes Induced by G Proteins. Co-overexpression of Gα-subunits and GPCRs will likely modify the local G protein environment sensed by GPCRs, leading to potential conformational changes in the GPCRs. These conformational changes induced by Gα-subunits can be reflected by a change in the pattern of SCAM-sensitive residues. Prior to determining potential changes in conformation, however, the basal MTSEA sensitivity patterns for the various cysteine mutants needed to be determined.

In initial studies, seven out of the 23 cysteine mutants in TM7 of KOR were identified as being significantly more sensitive to the MTSEA reagent than the C315$^{7.38}$S cysteine-less KOR as judged by an analysis of variance in HEK 293T cells: S310$^{7.33}$, F314$^{7.37}$, I316$^{7.39}$, A317$^{7.40}$, L318$^{7.41}$, G319$^{7.42}$, and Y320$^{7.43}$ (Figure 2a). Upon stable overexpression of $G\alpha_{16}$, an additional two residues—S311$^{7.34}$C and N326$^{7.49}$C—became sensitive (Figure 2a). Upon stable overexpression of the specific Gα-subunit $G\alpha_{i2}$, even more residues became sensitive (Y313$^{7.36}$, N322$^{7.45}$, S323$^{7.46}$, and L329$^{7.52}$). In addition, the absolute magnitude of average inhibition induced by the MTSEA reagent increased to 0.20 upon $G\alpha_{i2}$ overexpression (Table 2). In addition to a global change in TM7 residue sensitivity, there was an interesting switch for a critical residue essential for salvinorin A binding—Y313$^{7.36}$C—which changed from being insensitive to sensitive upon $G\alpha_{i2}$ overexpression.

Table 2: Changes in Inhibition upon Coupling of G Proteins $G\alpha_{16}$ and $G\alpha_{i2}$

	inhibition number	±inhibition number[a]	
	KOR	KOR·$G\alpha_{16}$	KOR·$G\alpha_{i2}$
	EL2 Mutants[a]		
C315$^{7.38}$S	0.05 ± 0.03	0.04	0.13
C315S-V205C	−0.13 ± 0.05	0.17	0.43
C315S-D206C	0.06 ± 0.09	0.01	0.14
C315S-V207C	−0.11 ± 0.08	0.21	0.21
C315S-I208C	0.24 ± 0.08	−0.17	0.07
C315S-E209C	0.07 ± 0.02	0.01	0.26
C315S-S211C	0.05 ± 0.02	0.15	0.22
C315S-L212C	0.57 ± 0.01	0.01	0.01
C315S-Q213C	0.003 ± 0.035	0.13	0.17
C315S-F214C	0.39 ± 0.09	0.05	0.08
C315S-P215C	0.22 ± 0.05	0.01	0.11
C315S-D216C	0.06 ± 0.04	0.05	0.14
average		0.06	0.17
	TM6 Mutants[b]		
C315$^{7.38}$S	0.05 ± 0.03	0.04	0.13
C315S-E297$^{6.58}$C	0.46 ± 0.003	0.15	0.13
C315S-V296$^{6.57}$C	0.28 ± 0.06	0.14	0.05
C315S-L295$^{6.56}$C	0.67 ± 0.07	−0.16	−0.16
C315S-I294$^{6.55}$C	0.65 ± 0.06	0.10	0.01
C315S-F293$^{6.54}$C	0.46 ± 0.06	0.03	0.18
C315S-I290$^{6.51}$C	0.72 ± 0.06	−0.01	−0.03
average		0.04	0.03
	TM7 Mutants[b]		
C315$^{7.38}$S	0.05 ± 0.03	0.04	0.13
C315S-L309$^{7.32}$C	−0.13 ± 0.09	0.37	0.28
C315S-S310$^{7.33}$C	0.32 ± 0.06	0.14	0.13
C315S-S311$^{7.34}$C	0.22 ± 0.06	0.17	0.24
C315S-Y312$^{7.35}$C	−0.17 ± 0.03	0.10	0.26
C315S-Y313$^{7.36}$C	0.28 ± 0.08	0.04	0.13
C315S-F314$^{7.37}$C	0.54 ± 0.04	0.05	0.18
C315S-I316$^{7.39}$C	0.46 ± 0.04	0.10	0.21
C315S-A317$^{7.40}$C	0.37 ± 0.03	0.02	0.19
C315S-L318$^{7.41}$C	0.46 ± 0.05	0.03	0.25
C315S-G319$^{7.42}$C	0.40 ± 0.06	−0.01	0.07
C315S-Y320$^{7.43}$C	0.65 ± 0.10	0	0.12
C315S-T321$^{7.44}$C	−0.01 ± 0.02	0.18	0.23
C315S-N322$^{7.45}$C	0.08 ± 0.04	0.13	0.34
C315S-S323$^{7.46}$C	0.12 ± 0.04	0.07	0.31
C315S-S324$^{7.47}$C	−0.07 ± 0.04	0.16	0.35
C315S-L325$^{7.48}$C	0.24 ± 0.04	−0.12	0.10
C315S-N326$^{7.49}$C	0.09 ± 0.04	0.26	0.30
C315S-P327$^{7.50}$C[c]			
C315S-I328$^{7.51}$C	−0.06 ± 0.07	0.20	0.36
C315S-L329$^{7.52}$C	0.14 ± 0.01	0.13	0.23
C315S-Y330$^{7.53}$C	0.14 ± 0.03	0.11	0.13
C315S-A331$^{7.54}$C	0.11 ± 0.02	0.03	0.16
C315S-F332$^{7.55}$C	0.18 ± 0.05	−0.02	−0.03
average		0.09	0.20

[a] ±inhibition number represents the difference of inhibition number between G protein-coupling and non-G coupling states. Negative sign (−) indicates decrease of inhibition number under G protein-coupling; positive sign (omitted in Table 2) indicates increase of inhibition number. [b] SCAM analysis revealed differential inhibition number changes in TM6, TM7, and EL2 of the KOR with various G protein-coupling. MTSEA was used to react specifically with cysteine side chains, and the modified cysteines show different inhibition ability of [^{3}H]diprenorphine (~0.2 nM) binding. The effects of MTSEA pretreatment on [^{3}H]diprenorphine binding were expressed as inhibition number. Data shown represent the mean ± SEM of three to six experiments. Inhibition number was calculated according to eq 1 in Materials and Methods. [c] [^{3}H]diprenorphine binding was undetectable for the C315$^{7.38}$S-P327$^{7.50}$C mutant.

Table 3: Second-Order Rate Constants (k, M^{-1} s^{-1}) of MTSEA Reaction with Cysteine Mutants of KOR

	K (M^{-1} s^{-1})[a]				
	KOR	KOR·Gα_{16}	KOR·Gα_{i2}	$k_{(KOR\cdot G\alpha_{16})}/k_{(KOR)}$	$k_{(KOR\cdot G\alpha_{i2})}/k_{(KOR)}$
C315S-S310$^{7.33}$C	8.5 ± 1.1	7.8 ± 2.4	7.7 ± 0.9	0.9	0.9
C315S-S311$^{7.34}$C	4.7 ± 1.0	7.1 ± 1.3	4.7 ± 0.3	1.5	1.0
C315S-Y313$^{7.36}$C	5.8 ± 1.7	7.1 ± 1.4	11.1 ± 3.2	1.2	1.9
C315S-F314$^{7.37}$C	4.2 ± 0.5	9.7 ± 2.4	6.8 ± 1.7	2.3	1.6
C315S-I316$^{7.39}$C	6.1 ± 1.5	14.1 ± 3.1	7.9 ± 2.1	2.3	1.3
C315S-A317$^{7.40}$C	4.7 ± 1.0	5.9 ± 1.3	4.2 ± 1.4	1.3	0.9
C315S-L318$^{7.41}$C	4.5 ± 0.9	5.0 ± 1.1	8.1 ± 1.6	1.1	1.8
C315S-G319$^{7.42}$C	5.8 ± 1.4	5.6 ± 1.1	4.7 ± 1.4	1.0	0.8
C315S-Y320$^{7.43}$C	5.2 ± 1.8	5.3 ± 1.7	8.6 ± 0.8	1.0	1.7
C315S-N322$^{7.45}$C	10.1 ± 3.5	5.3 ± 1.1	11.6 ± 3.2	0.5	1.2
C315S-S323$^{7.46}$C	4.7 ± 1.3	5.1 ± 0.8	6.1 ± 1.2	1.1	1.3
C315S-N326$^{7.49}$C	4.9 ± 0.8	15.2 ± 4.4	5.4 ± 2.0	3.1	1.1
C315S-L329$^{7.52}$C	13.5 ± 4.3	7.3 ± 2.2	6.7 ± 1.5	0.5	0.5

[a] Selected rates of cysteine-mutant reaction with MTSEA were examined. Cells were treated with four concentrations of MTSEA, followed by quenching, washing, and [^{3}H]diprenorphine binding. The second-order rate constants (k) were determined in triplicate. Data represent in mean ± SEM of three to eight independent experiments.

Table 4: Differential Effects of G Protein-Coupling on Agonists (Salvinorin A, U69593, and Dynorphin A (1-13)) Binding Affinities (K_i, nM)

	radioactive label [^{3}H]diprenorphine					
	salvinorin A		U69593		dynorphin A (1-13)	
tested agonists[a]	K_i (nM)[b]	ratio[c]	K_i (nM)[b]	ratio[c]	K_i (nM)[b]	ratio[c]
KOR	33 ± 8		69 ± 12		0.94 ± 0.21	
KOR·Gα_{16}	13 ± 4[d]	2.5	59 ± 8	1.2	0.98 ± 0.56	1.0
KOR·Gα_{i2}	8.6 ± 1.5[d]	3.8	25 ± 6[d]	2.8	1.5 ± 0.7	0.6
	radioactive label [^{3}H]U69593					
	salvinorin A		U69593		dynorphin A (1-13)	
tested agonists[a]	K_i (nM)[b]	ratio[c]	K_i (nM)[b]	ratio[c]	K_i (nM)[b]	ratio[c]
KOR	0.80 ± 0.33		1.0 ± 0.2		0.19 ± 0.06	
KOR·Gα_{16}	0.045 ± 0.019[d]	18	0.81 ± 0.13	1.2	0.22 ± 0.07	0.9
KOR·Gα_{i2}	0.12 ± 0.06[d]	6.7	0.89 ± 0.15	1.1	0.21 ± 0.02	0.8

[a] Salvinorin A and U69593 are small-molecule agonists (MW ~400 Da); dynorphin A (1-13) is the short form of the endogenous peptide agonist (MW ~1600 Da). [b] Affinity constants (K_i, nM) of the different agonists were determined in competition binding assays with [^{3}H]diprenorphine (antagonist) or [^{3}H]U69593 (agonist) and increasing concentrations of agonists (from 10^{-5} to 10^4 nM). Data represent three to six independent experiments as mean ± SEM. [c] Ratio is $K_{i(KOR)}/K_{i(KOR\cdot G\alpha_{16})}$ or $K_{i(KOR)}/K_{i(KOR\cdot G\alpha_{i2})}$. [d] $p < 0.05$ vs KOR.

For TM6, only residues that had previously been determined to be sensitive by other investigators were tested (*24*). It was found that the upper part of TM6 displayed only a limited change in the absolute amount of sensitivity from 0.04 in Gα_{16} cells to 0.03 in Gα_{i2} cells (Table 2). An interesting observation was that V296$^{6.57}$C became insensitive after Gα_{i2} overexpression (Figure 2b). These findings are consistent with a model that implies that V296$^{6.57}$ is a half-turn from I294$^{6.55}$ and is facing either other TMs or lipids. EL2 also presented a significant change in overall inhibition (0.06 for Gα_{16} and 0.17 for Gα_{i2} respectively), with two residues L212 and F214 being identified as SCAM-sensitive residues, being somewhat more sensitive in the G protein overexpression settings (Table 2 and Figure 2c).

Second-Order Rate Constants of MTSEA Reactions with Sulfhydryls. The estimation of second-order rate constants was performed by using the pseudo-first-order method (see Materials and Methods). Briefly, the extent of reaction after a fixed time with four concentrations of MTSEA (all in excess over the reactive sulfhydryls) was determined. For kinetic studies, a slight fluctuation of reaction rate will affect the inhibition number dramatically due to the exponential relationship between the reaction rate and the inhibition effect. TM7 cysteine mutants were chosen for a kinetics study since they displayed larger average inhibition changes (0.2 under Gα_{i2} overexpression as discussed previously). The reaction rate varied significantly depending on the milieu ranging from 0.5- to 3.1-fold changes (Table 3) upon Gα_{16} overexpression. Most of the cysteine mutants displayed no change in reactivity or became more reactive, with two notable exceptions (N322$^{7.45}$C and L329$^{7.52}$C). For Gα_{i2} conditions, a different pattern of reactivity was observed. Some mutants showed increased reactivity (Y313$^{7.36}$C, F314$^{7.37}$C, L318$^{7.41}$C, and Y320$^{7.43}$C), while L329$^{7.52}$C displayed a decreased reactivity. This kinetic method was not applied to the sensitive residues of TM6 and EL2. Generally, the second-order rate data were consistent with the SCAM data, showing a distinct pattern of reaction rate for the sensitive mutants upon different G protein-coupling (*vide infra*).

We also examined the effect of preincubation with naloxone on protection against the MTSEA reagent. Our results were essentially similar to those previously published for both sensitive and insensitive residues (data not shown) (*23*, *24*).

Conformational Changes Induced by G Protein-Coupling Have Significant Effects on Agonist Affinities. To examine the consequences of these conformational changes induced

by various G protein backgrounds, three KOR agonists (salvinorin A, U69593, and dynorphin A (1-13)) were tested against wild-type KOR transiently expressed in the three cell systems (Figure 1). Two different radioactive ligands (the antagonist [^{3}H]diprenorphine and the agonist [^{3}H]U69593) were also used. In both the Gα_{16} and the Gα_{i2} environments, salvinorin A and U69593 demonstrated significantly enhanced affinities (Table 4), although, surprisingly, the endogenous peptide dynorphin A (1-13)'s affinity was almost unchanged. Using [^{3}H]U69593 revealed a differential preference between salvinorin A and U69593 as well. The largest effect (18-fold) was seen for salvinorin A in the Gα_{16} background using [^{3}H]U69593 as the radioligand.

KOR Modeling. The proposed model for the activated form of the hKOR, as recognized by the agonist salvinorin A, is shown in Figure 3a,b. Figure 4 illustrates the axial and radial distribution of side chains in TM6 and TM7 for those positions that were tested in the SCAM/[^{3}H]diprenorphine binding experiments. The model shown in Figure 3b, unlike earlier proposed hKOR models (*25*, *27*) such as the one depicted in Figure 3a, is based on the recently determined crystal structure of photoactivated bovine rhodopsin (*22*). The side chain conformations in the TM helical regions of the dark state (i.e., PDB ID 1U19 (*29*)) and activated rhodopsin crystals are essentially the same; however, there is a subtle but distinct difference in the positions of the TM helices relative to one another. In the activated crystal form, TM3 and TM6 are roughly 1 Å further apart from one another in the intracellular region as compared to the dark state. On the basis of the experimental findings reported here and elsewhere (*13*, *16*), the binding of the G protein complex is thought to induce an active or active-like state that is more conducive to the binding of agonists than is the inactive state. This change upon activation (or binding of G protein) of the GPCR effectively extends the binding pocket to include a narrow region bounded by the intracellular regions of TM2, TM3, TM6, and TM7. As shown in Figure 3b, the residues of TM7 that line this narrow extended binding site are those residues that, under conditions of G protein overexpression, were found to significantly affect the binding of [^{3}H]-diprenorphine when those positions were subjected to the SCAM procedure. This implies that these residues become accessible to the relatively small MTSEA reagent when G proteins are overexpressed, and this is reflected in the activated rhodopsin-based model. The rate at which MTSEA reacts with the sulfhydryl groups at various positions along TM7 in the Gα-overexpressed systems relative to the non-Gα-overexpressed system was visualized (see Figure 5). With the exception of N326$^{7.49}$ in the Gα_{16}-overexpressed system, residue positions closer to the extracellular side (i.e., top) of the KOR react more rapidly than do those near the intracellular side when Gα-proteins are overexpressed.

EL2 Residues Involved in Salvinorin A Binding. It has been previously suggested that EL2 is critical for salvinorin A-KOR binding, although no residues have been thus far identified. As the sensitive residues identified by SCAM, L212 and F214 have great potential to be critical residues for salvinorin A binding. Mutagenesis was applied to them and because they are quite bulky hydrophobic residues, L212A and F214A were constructed to examine a potential steric hindrance effect. Interestingly, alanine substitution at L212 and F214 enhanced salvinorin A affinity K_i values (1.7

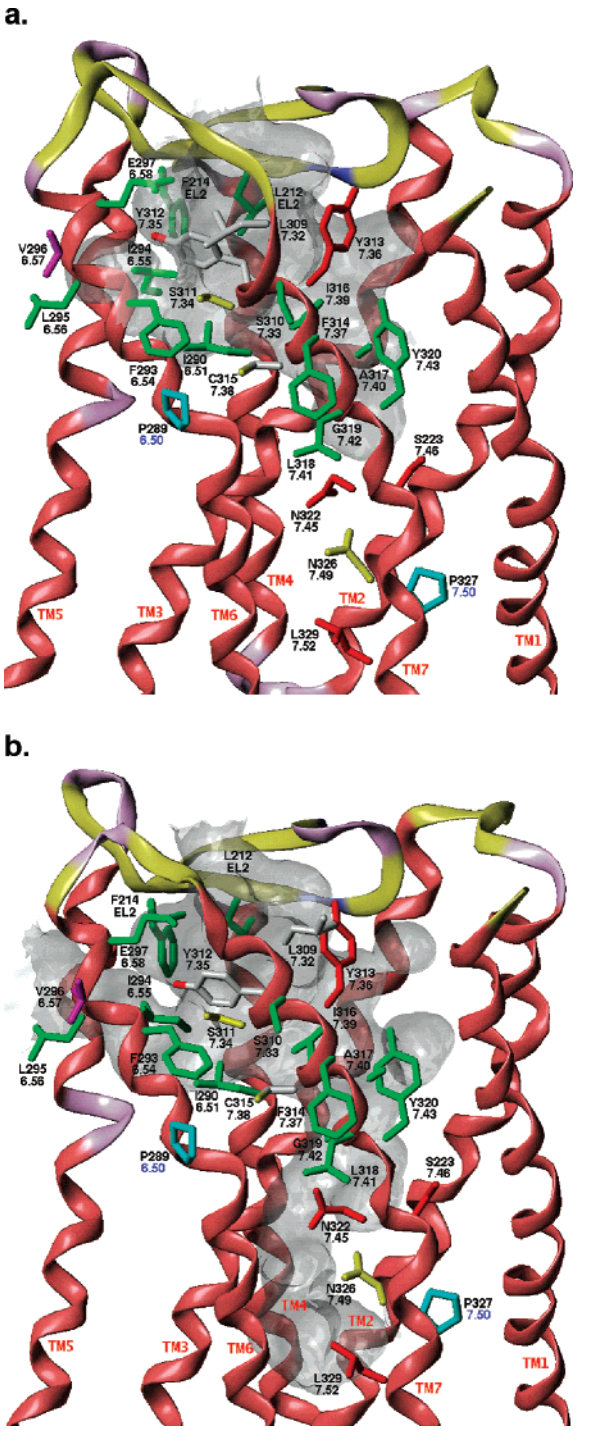

FIGURE 3: (a) Ribbon diagram of an earlier hKOR model derived from the dark rhodopsin crystal structure. (b) Ribbon diagram of the activated hKOR model derived from the light rhodopsin crystal structure. Ribbons are color-coded based on secondary structure: red = α-helix, blue = *β*-strand, violet = turn, and yellow = coil. Selected side chains of residues in TM6, TM7, and EL2 whose positions were tested for [^{3}H]diprenorphine inhibition are shown as capped sticks. Side chain color-coding indicates the conditions under which significantly altered [^{3}H]diprenorphine binding occurred relative to the C315$^{7.38}$S reference (see Figure 2a−c): green = KOR, KOR·Gα_{16}, and KOR·Gα_{i2}; yellow = KOR·Gα_{16} and KOR·Gα_{i2}; red = KOR·Gα_{i2} only; magenta = KOR and KOR·Gα_{16}. Side chains containing gray atoms did not significantly alter [^{3}H]diprenorphine binding under any of the three conditions or were not tested (i.e., C315$^{7.38}$). Cyan indicates conserved proline residues. A Connolly channel plot delineating the binding pocket in each receptor is shown as a transparent gray surface (probe radius = 1.4 Å). TM6 and TM7 are closest to the viewer.

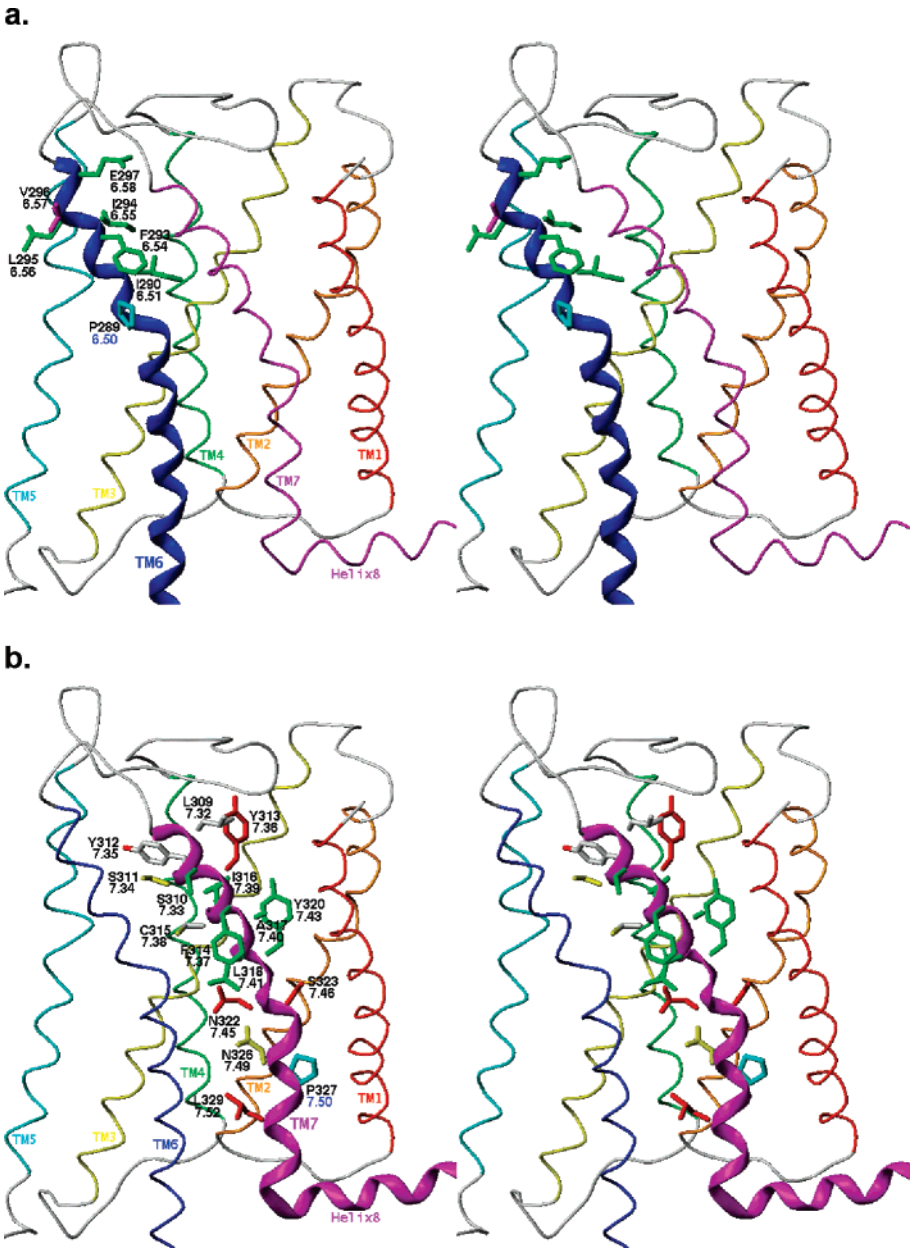

FIGURE 4: Stereoviews (relaxed, separation = 4.0° and opsis = 6.0°) of the activated KOR model, highlighting the residues of TM6 and TM7 that were tested in the SCAM/diprenorphine binding experiment. (a) TM6 and (b) TM7. The side chains depicted and their color-codes are the same as in Figure 3b.

and 1.0 nM, respectively; Table 5), while alanine mutagenesis of neighboring residues (S211A and Q214A) had no effect. According to our recent model, the EL2 dips down into the hKOR binding pocket (Figure 3), placing L212 and F214 into the binding pocket. Some other critical residues ($I294^{6.55}A$ and $Q115^{2.60}A$) were also examined. $Q115^{2.60}A$ decreased the K_i value 17-fold, consistent with the results reported by Kane et al. (*30*). The role of $Q115^{2.60}$ in salvinorin A binding is not well-understood; however, a hydrogen bond with the furan oxygen of salvinorin A is suggested by our latest models (Figure 3a,b).

DISCUSSION

Our major finding is that $G\alpha_{i2}$ and $G\alpha_{16}$ differentially modulate the conformation of a prototypical family A GPCR—the κ-opioid receptor (KOR). It was discovered that when $G\alpha_{i2}$ and $G\alpha_{16}$ were overexpressed together with KOR, a differential pattern of cysteine accessibility to MTSEA was observed. In conjunction with these apparent changes in the KOR conformation, there was a selective alteration in salvinorin A's affinity. These results are consistent with the hypothesis that Gα-subunits differentially interact with GPCRs in the absence of agonists and that such interactions lead to conformational changes that are reflected in altered ligand affinities.

In the way it is applied here, SCAM is a biochemical method capable of detecting averaged receptor conformations in a defined time period (5 min in these studies). Both static conformations as well as averaged conformational fluctuations during the period the system is exposed to the MTSEA reagent will be reflected in altered cysteine reactivity. The final SCAM pattern of MTSEA sensitivity thus represents a summary of the multiplicity of conformations of KOR in the presence and absence of Gα-subunit overexpression. Our

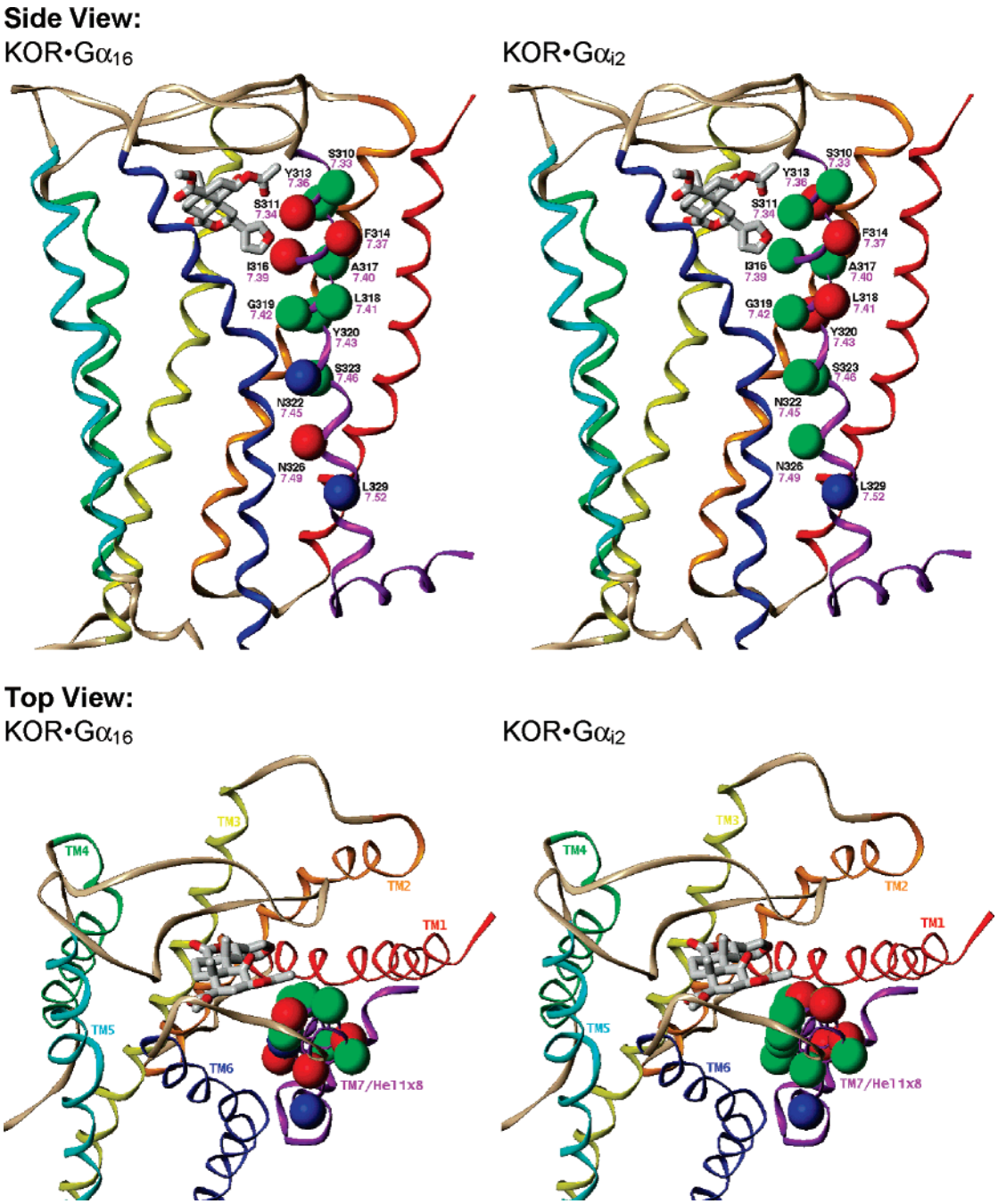

FIGURE 5: Second-order rate constants (k, M^{-1} s^{-1}) revealed a directional preference and α-helical periodicity. The ratios ($k_{(G\alpha_{16})}/k_{(non-G\alpha)}$ or $k_{(G\alpha_{i2})}/k_{(non-G\alpha)}$) of MTSEA reaction rates upon G protein-coupling were divided into three subgroups, highlighted by labeling the α-carbon with different colors: Red: ratio > 1.5; green, 0.5 < ratio ≤ 1.5; and blue, ratio ≤ 0.5. All of the residues presented inhibited the binding of [^{3}H]diprenorphine by greater than 35% upon $G\alpha_{i2}$ coupling and were significantly different from the background C315$^{7.38}$S in the SCAM pattern (see Figure 2a). The KOR backbone is represented by a thin ribbon in which the individual TMs are color-coded (TM1 = red; TM2 = orange; TM3 = yellow; TM4 = green; TM5 = cyan; TM6 = blue; and TM7/helix 8 = violet), and salvinorin A is rendered as capped sticks (carbon = gray and oxygen = red).

data in Table 2 demonstrate that the averaged inhibition values of SCAM-sensitive residues are significantly changed by Gα-subunit overexpression—especially by $G\alpha_{i2}$. This change in MTSEA sensitivity in the absence of agonist binding strongly supports the notion that Gα-subunits can induce conformational changes in GPCRs. It has been conventionally postulated that following agonist exposure, GPCR conformations are altered. Indeed, some novel methodological approaches have recently demonstrated agonist-induced conformational changes in several GPCRs (*31*−*33*). To our knowledge, our results are the first to demonstrate that G proteins can alter GPCR conformations in the absence of ligand and, in addition, these findings are consistent with a growing literature suggesting the existence of precoupled GPCR-G protein complexes (*13*, *34*, *35*).

In this study, the patterns of residue accessibility (see Figure 2a−c) were rationalized via the comparison of our hKOR model with inactive and active rhodopsin structures. The analysis of these residue accessibility patterns was divided into three regions of the KOR. These regions consisted of (a) residues at the extracellular end of TM7, (b) the regions comprising the bulk of the extracellular

Table 5: Affinity (K_i, nM) of Salvinorin a Binding to Wild-Type KOR and Mutants

	K_d (nM)[a]	B_{max} (pmol/mg)[a]	$K_{d(mutant)}/K_{d(WT)}$	K_i (nM)[b]	$K_{i(mutant)}/K_{i(WT)}$
KOR-WT	0.46 ± 0.10	2.0 ± 0.4		33 ± 8	
S211A	0.47 ± 0.10	2.7 ± 0.8	1.0	38 ± 5	1.2
L212A	0.28 ± 0.07	0.27 ± 0.08	0.6	1.7 ± 1.0	0.05
Q213A	0.51 ± 0.15	0.76 ± 0.04	1.1	40 ± 12	1.2
F214A	0.46 ± 0.22	0.8 ± 0.7	1.0	1.0 ± 0.1	0.03
$I294^{6.55}A$	0.53 ± 0.18	0.9 ± 0.8	1.2	12 ± 6	0.4
$E297^{6.58}A$	0.91 ± 0.08	1.8 ± 1.2	2.0	15 ± 3	0.5
$Q115^{2.60}A$	0.65 ± 0.10	2.5 ± 1.7	1.4	556 ± 231	17

[a] Saturation binding of [^{3}H]diprenorphine to the wild-type and mutants was performed according to the procedure in Materials and Methods. Data represent the mean ± SEM of two to four independent experiments. [b] Affinity constants (K_i) of the different compounds were determined in competition binding assays with [^{3}H]diprenorphine and increasing concentrations of salvinorin A (from 10^{-5} to 10^4 nM). Data represent the mean ± SEM of two to four independent experiments.

portions of both TM6 and TM7, and (c) in and near the NPxxY region of TM7.

Residues $L309^{7.32}$ to $Y313^{7.36}$ are located at the extracellular end of TM7. $L309^{7.32}$ and $Y312^{7.35}$ were never accessible (or undetectable by inhibition of binding), while $S310^{7.33}$ was always accessible and significantly affected the binding of diprenorphine. $S311^{7.34}$ became accessible upon binding of $G\alpha_{16}$ or $G\alpha_{i2}$. $Y313^{7.36}$ became accessible only on overexpression of $G\alpha_{i2}$. The reasons for this pattern were not clear, but it appears that $Y313^{7.36}$ could easily interact with residues of EL2, causing it to remain partially sterically shielded under ordinary (normal G protein expression level) conditions based on a comparison of the inactive and photoactivated crystal structures of bovine rhodopsin. In the case of rhodopsin, photoactivation produced a subtle movement of TM7 away from EL2. Presumably, a similar conformational change could take place upon coupling and/or activation of the hKOR by $G\alpha_{i2}$ with the movement of TM7 with respect to EL2, making the 7.36 position more accessible.

In the regions comprising the extracellular portions of both TM6 and TM7, there are contiguous sequences of amino acids ($F293^{6.54}$ to $L299^{6.60}$ and $F314^{7.37}$ to $Y320^{7.43}$) that were accessible. This cluster pattern of accessibility has previously been observed in TM6 and TM7 for the MOR and DOR as well as the KOR (*23*, *24*). To date, this pattern of accessibility has been generally attributed to the inherent flexibility of the helix and/or to the permeability of the MTSEA reagent through the lipid membrane (*36*). Analysis of SCAM second-order reaction rates had been used to predict which residues most likely (or most often) face the interior of the binding cavity (*24*). Some of the reaction rates reported here were lower than previously reported (*23*, *24*) and are likely due to differences in experimental techniques. In addition, the reactivity of individual residues (in TM7) did appear to indicate a directional preference and α-helical periodicity (see Figure 5).

An interesting pattern of accessibility was found near the NPxxY region of TM7. $Y320^{7.43}$, the site of retinal attachment in rhodopsin, is also the locus of one to two turns of the more tightly wound 3_{10} helix. The kink in TM7 also occurred one turn below $Y320^{7.43}$. On the intracellular side of $Y320^{7.43}$, residues were accessible and inhibited the binding of [^{3}H]diprenorphine by greater than 40% only when $G\alpha_{i2}$ was overexpressed. It is difficult to visualize, in the case of $G\alpha_{16}$ expression, how $N326^{7.49}$ was accessible yet $N322^{7.45}$ and $S323^{7.46}$ (one turn above) were inaccessible. One possible explanation is that when $N322^{7.45}$ (and perhaps $S323^{7.46}$, depending on the rotational disposition of TM7) was mutated to cysteine, a disulfide bond could be formed with an adjacent cysteine residue on TM6 ($C286^{6.47}$), rendering it unreactive to the MTSEA reagent.

An intriguing pattern emerged when the SCAM-sensitive residues in TM6 and TM7 were evaluated. The overaccessibility patterns are likely due to the disorder of this region of the helix; also, dynamic movements and the proline kink at $P327^{7.50}$ may play a role. In a recent study (*23*), Xu et al. also suggested that the large distance between TM1 and TM7 may allow MTSEA to penetrate the KOR TM1−TM7 interface to react with substituted cysteines. However, some of the most sensitive residues are not directly facing to the binding pocket (Figure 2a). Further study is necessary to clarify this. The most sensitive residues on TM6 ($E297^{6.58}$, $I294^{6.55}$, and $I290^{6.51}$) and EL2 (L212 and F214) point the binding pocket, which is consistent with the current model.

A pseudo-first-order method was used for obtaining the second-order rate of MTSEA reactions. For the 13 TM7 cysteine mutants examined (Table 3), most ($S311^{7.34}$C, $Y313^{7.36}$C, $F314^{7.37}$C, $I316^{7.39}$C, $L318^{7.41}$C, $Y320^{7.43}$C, and $N326^{7.49}$C) have increased or unchanged reaction rates under either $G\alpha_{i2}$ or $G\alpha_{16}$ overexpression systems, which are consistent with the SCAM data. $S311^{7.34}$C, $I316^{7.39}$C, and $N326^{7.49}$C show enhancement under $G\alpha_{16}$ overexpression but not $G\alpha_{i2}$. The differences may be caused by an unfavorable local environment change presented in the new conformations in the $G\alpha_{i2}$ overexpression system but could also be caused by the proposed inherent flexibility of the extracellular portion of TM7. Since the conformational change is not dramatic and those residues are located in the upper part of the helix, a longer time exposure of MTSEA could compensate and reveal a high SCAM inhibition. $N322^{7.45}$C, $S323^{7.46}$C, and $L329^{7.52}$C, whose access to MTSEA is presumably less than that of more extracellularly located residues (even under conditions of G protein overexpression) and whose kinetic reaction rates are generally less than those of more extracellularly located residues, can still significantly affect the binding of diprenorphine when these mutants are reacted with MTSEA. $L329^{7.52}$C is furthest down in the pocket and theoretically least accessible to MTSEA (see Figure 3b). It should be mentioned that the mechanism by which the MTSEA reaches buried cysteine residues such as $C329^{7.52}$ is not perfectly clear, as some studies have indicated that MTSEA is lipid membrane-permeable (*36*). In general, the reaction rates with G protein overexpression are within

0.5−3.1-fold of the corresponding non-G protein overexpression systems, and there is no large increase of rate observed between different mutants.

The reactivity of TM7 cysteine mutants demonstrated a directional preference and α-helical periodicity (Figure 5). Figure 5 shows that TM7 may undergo a modest counterclockwise rotation (viewed from the extracellular side) when in the presence of overexpressed $G\alpha_{i2}$, but the rotational preference for TM7 of the $G\alpha_{16}$-overexpressed KOR is less clear; its pattern of reactivity is possibly due to the effects of MTSEA membrane permeability and/or rotational flexibility. However, it seems reasonable to expect that the KOR presents a consistent and complimentary receptor conformation to approaching agonists, at least in the case of salvinorin A and U69593, whose binding affinities increased by roughly the same amount in both $G\alpha_{16}$- and $G\alpha_{i2}$-overexpressed systems (see Table 4).

As compared to TM6 and TM7, the pattern of EL2 is relatively simple, with only two residues (L212 and F214) next to C210—which likely forms a disulfide bond with C131—identified as sensitive. The residues next to C210, L212 and F214, are likely not to be as conformationally flexible as the other loop residues and are more likely to present their side chains in a fixed direction pointing down into the binding pocket. Similar observations were reported for the D_2-dopamine receptor EL2 (*37*), where two residues (I184 and N186) were found to be SCAM-sensitive. In the D_2 receptor, I184 and N186 are adjacent to the disulfide bond-forming C182, just as L212 and F214 are adjacent to C210 in the KOR. The KOR modeling studies presented here led to the prediction that L212 and F214 would cause a large steric hindrance for ligand binding to KOR. A reasonable prediction was that a smaller hydrophobic residue will lessen the blockage and potentiate ligand binding. The profound increase of salvinorin A binding for KOR mutants (L212A and F214A) supports this model (Table 5).

In summary, our findings are consistent with the hypothesis that Gα-subunits differentially modulate the conformation of GPCRs, leading to distinctive patterns of ligand selectivity. Our data also support an emerging body of data demonstrating precoupling of GPCRs and G proteins. Finally, our data provide evidence for the hypothesis that G protein-induced conformational changes lead to differential ligand selectivities and patterns of efficacy and provide biophysical evidence in support of the functional selectivity hypothesis of GPCR actions.

ACKNOWLEDGMENT

We thank Drs. Vernon Anderson, Paul Ernsberger, Martin Snider, and Timothy A. Vortherms for informative discussions and Ryan Strachan and Atheir Abbas for careful review of the manuscript.

REFERENCES

1. Berg, K. A., Maayani, S., Goldfarb, J., Scaramellini, C., Leff, P., and Clarke, W. P. (1998) Effector Pathway-Dependent Relative Efficacy at Serotonin Type 2A and 2C Receptors: Evidence for Agonist-Directed Trafficking of Receptor Stimulus, *Mol. Pharmacol. 54*, 94−104.
2. Gettys, T. W., Fields, T. A., and Raymond, J. R. (1994) Selective Activation of Inhibitory G-Protein α-Subunits by Partial Agonists of the Human $5\text{-}HT_{1A}$ Receptor, *Biochemistry 33*, 4283−4290.
3. Gray, J. A., Sheffler, D. J., Bhatnagar, A., Woods, J. A., Hufeisen, S. J., Benovic, J. L., and Roth, B. L. (2001) Cell-Type Specific Effects of Endocytosis Inhibitors on $5\text{-Hydroxytryptamine}_{2A}$ Receptor Desensitization and Resensitization Reveal an Arrestin-, GRK2-, and GRK5-Independent Mode of Regulation in Human Embryonic Kidney 293 Cells, *Mol. Pharmacol. 60*, 1020−1030.
4. Raymond, J. R., Olsen, C. L., and Gettys, T. W. (1993) Cell-Specific Physical and Functional Coupling of Human $5\text{-}HT_{1A}$ Receptors to Inhibitory G Protein α-Subunits and Lack of Coupling to $G_{s\alpha}$, *Biochemistry 32*, 11064−11073.
5. Roth, B. L., and Chuang, D.-M. (1987) Multiple Mechanisms of Serotonergic Signal Transduction, *Life Sci. 41*, 1051−1064.
6. Aronin, N., and DiFiglia, M. (1992) The Subcellular Localization of the G-Protein $G_{i\alpha}$ in the Basal Ganglia Reveals Its Potential Role in Both Signal Transduction and Vesicle Trafficking, *J. Neurosci. 12*, 3435−3444.
7. Giesberts, A. N., van Ginneken, M., Gorter, G., Lapetina, E. G., Akkerman, J.-W. N., and van Willigen, G. (1997) Subcellular Localization of α-Subunits of Trimeric G-Proteins in Human Platelets, *Biochem. Biophys. Res. Commun. 234*, 439−444.
8. Kawai, Y., and Arinze, I. J. (1996) Differential Localization and Development-Dependent Expression of G-Protein Subunits, Goα and G*β*, in Rabbit Heart, *J. Mol. Cell. Cardiol. 28*, 1555−1564.
9. Eglen, R. M. (2005) Emerging Concepts in GPCR Function—The Influence of Cell Phenotype on GPCR Pharmacology, *Proc. West. Pharmacol. Soc. 48*, 31−34.
10. Krumins, A. M., and Gilman, A. G. (2006) Targeted Knockdown of G Protein Subunits Selectively Prevents Receptor-Mediated Modulation of Effectors and Reveals Complex Changes in Non-targeted Signaling Proteins, *J. Biol. Chem. 281*, 10250−10262.
11. Tinker, A. (2006) The Selective Interactions and Functions of Regulators of G-protein Signaling, *Sem. Cell Dev. Biol. 17*, 377−382.
12. Urban, J. D., Clarke, W. P., von Zastrow, M., Nichols, D. E., Kobilka, B., Weinstein, H., Javitch, J. A., Roth, B. L., Christopoulos, A., Sexton, P. M., Miller, K. J., Spedding, M., and Mailman, R. B. (2007) Functional Selectivity and Classical Concepts of Quantitative Pharmacology, *J. Pharmacol. Exp. Ther. 320*, 1−13.
13. Nobles, M., Benians, A., and Tinker, A. (2005) Heterotrimeric G Proteins Precouple With G Protein-Coupled Receptors in Living Cells, *Proc. Natl. Acad. Sci. U.S.A. 102*, 18706−18711.
14. Rebois, R. V., Robitaille, M., Galés, C., Dupré, D. J., Baragli, A., Trieu, P., Ethier, N., Bouvier, M., and Hébert, T. E. (2006) Heterotrimeric G Proteins form Stable Complexes with Adenylyl Cyclase and Kir3.1 Channels in Living Cells, *J. Cell Sci. 119*, 2807−2818.
15. Devanathan, S., Yao, Z., Salamon, Z., Kobilka, B., and G., T. (2004) Plasmon-Waveguide Resonance Studies of Ligand Binding to the Human β_2-Adrenergic Receptor, *Biochemistry 43*, 3280−3288.
16. Galandrin, S., and Bouvier, M. (2006) Distinct Signaling Profiles of β_1 and β_2 Adrenergic Receptor Ligands toward Adenylyl Cyclase and Mitogen-Activated Protein Kinase Reveals the Pluridimensionality of Efficacy, *Mol. Pharmacol. 70*, 1575−1584.
17. Alousi, A., Jasper, J. R., Insel, P. A., and Motulsky, H. J. (1991) Stoichiometry of Receptor-G_s-adenylate Cyclase Interactions, *FASEB J. 5*, 2300−2303.
18. Kenakin, T. (1997) Differences between Natural and Recombinant G Protein-Coupled Receptor Systems with Varying Receptor/G Protein Stoichiometry, *Trends Pharmacol. Sci. 18*, 456−464.
19. Connor, M., and Christie, M. J. (1999) Opioid Receptor Signaling Mechanisms, *Clin. Exp. Pharmacol. Physiol. 26*, 493−499.
20. Lee, J. W. M., Joshi, S., Chan, J. S. C., and Wong, Y. H. (1998) Differential Coupling of μ-, δ-, and κ-Opioid Receptors to $G\alpha_{16}$-Mediated Stimulation of Phospholipase C, *J. Neurochem. 70*, 2203−2211.
21. Javitch, J. A., Fu, D., Liapakis, G., and Chen, J. (1997) Constitutive Activation of the β_2 Adrenergic Receptor Alters the Orientation of Its Sixth Membrane-Spanning Segment, *J. Biol. Chem. 272*, 18546−18549.
22. Salom, D., Lodowski, D. T., Stenkamp, R. E., Le Trong, I., Golczak, M., Jastrzebska, B., Harris, T., Ballesteros, J. A., and Palczewski, K. (2006) Crystal Structure of a Photoactivated Deprotonated Intermediate of Rhodopsin, *Proc. Natl. Acad. Sci. U.S.A. 103*, 16123−16128.
23. Xu, W., Campillo, M., Pardo, L., de Riel, J. K., and Liu-Chen, L.-Y. (2005) The Seventh Transmembrane Domains of the δ and

κ Opioid Receptors Have Different Accessibility Patterns and Interhelical Interactions, *Biochemistry 44*, 16014−16025.
24. Xu, W., Li, J., Chen, C., Huang, P., Weinstein, H., Javitch, J. A., Shi, L., de Riel, J. K., and Liu-Chen, L.-Y. (2001) Comparison of the Amino Acid Residues in the Sixth Transmembrane Domains Accessible in the Binding-Site Crevices of μ, δ, and κ Opioid Receptors, *Biochemistry 40*, 8018−8029.
25. Vortherms, T. A., Mosier, P. D., Westkaemper, R. B., and Roth, B. L. (2007) Differential Helical Orientations among Related G Protein-Coupled Receptors Provide a Novel Mechanism for Selectivity: Studies with Salvinorin A and the κ-Opioid Receptor, *J. Biol. Chem. 282*, 3146−3156.
26. Cantescu, A. A., Shelenkov, A. A., and Dunbrack, R. L., Jr. (2003) A Graph-Theory Algorithm for Rapid Protein Side-Chain Prediction, *Protein Sci. 12*, 2001−2014.
27. Yan, F., Mosier, P. D., Westkaemper, R. B., Stewart, J., Zjawiony, J. K., Vortherms, T. A., Sheffler, D. J., and Roth, B. L. (2005) Identification of the Molecular Mechanisms by Which the Diterpenoid Salvinorin A Binds to κ-Opioid Receptors, *Biochemistry 44*, 8643−8651.
28. Xu, W., Chen, C., Huang, P., Li, J., de Riel, J. K., Javitch, J. A., and Liu-Chen, L.-Y. (2000) The Conserved Cysteine 7.38 Residue Is Differentially Accessible in the Binding-Site Crevices of the μ, δ, and κ Opioid Receptors, *Biochemistry 39*, 13904−13915.
29. Okada, T., Sugihara, M., Bondar, A.-N., Elstner, M., Entel, P., and Buss, V. (2004) The Retinal Conformation and Its Environment in Rhodopsin in Light of a New 2.2 Å Crystal Structure, *J. Mol. Biol. 342*, 571−583.
30. Kane, B. E., Nieto, M. J., McCurdy, C. R., and Ferguson, D. M. (2006) A Unique Binding Epitope for Salvinorin A, a Non-nitrogenous Kappa Opioid Receptor Agonist, *FEBS Lett. 273*, 1966−1974.
31. Buck, E., and Wells, J. A. (2005) Disulfide Trapping to Localize Small-Molecule Agonists and Antagonists for a G Protein-Coupled Receptors, *Proc. Natl. Acad. Sci. U.S.A. 102*, 2719−2724.
32. Elling, C. E., Frimurer, T. M., Gerlach, L.-O., Jorgensen, R., Holst, B., and Schwartz, T. W. (2006) Metal Ion Site Engineering Indicates a Global Toggle Switch Model for Seven-Transmembrane Receptor Activation, *J. Biol. Chem. 281*, 17337−17346.
33. Han, S.-J., Hamdan, F. F., Kim, S.-K., Jacobsen, K. A., Bloodworth, L. M., Li, B., and Wess, J. (2005) Identification of an Agonist-Induced Conformational Change Occurring Adjacent to the Ligand-Binding Pocket of the M_3 Muscarinic Acetylcholine Receptor, *J. Biol. Chem. 280*, 34849−34858.
34. Galés, C., Rebois, R. V., Hogue, M., Trieu, P., Breit, A., Hérbert, T. E., and Bouvier, M. (2005) Real-Time Monitoring of Receptor and G-Protein Interactions in Living Cells, *Nat. Methods 2*, 177−184.
35. Neubig, R. R., Gantzos, R. D., and Thompsen, W. J. (1988) Mechanism of Agonist and Antagonist Binding to α_2 Adrenergic Receptors: Evidence for a Precoupled Receptor-Guanine Nucleotide Protein Complex, *Biochemistry 27*, 2374−2384.
36. Holmgren, M., Liu, Y., Xu, Y., and Yellen, G. (1996) On the Use of Thiol-Modifying Agents to Determine Channel Topology, *Neuropharmacology 35*, 797−804.
37. Shi, L., and Javitch, J. A. (2004) The Second Extracellular Loop of the Dopamine D_2 Receptor Lines the Binding-Site Crevice, *Proc. Natl. Acad. Sci. U.S.A. 101*, 440−445.

BI701476B